doi:10.1017/S1431927622002331
Microsc. Microanal. 28 (Suppl 1), 2022

Exploring the 3D Resolution of Parallax Phase Reconstruction from 4D STEM: A Dopant Depth Case Study

E.W.C. Terzoudis-Lumsden[1]*, T.C. Petersen[2], H.G. Brown[3], P.M. Pelz[4,5.], C. Ophus[4] and S.D. Findlay[1]

[1.] School of Physics and Astronomy, Monash University, Melbourne, VIC, Australia
[2.] Monash Centre for Electron Microscopy, Monash University, Melbourne, VIC, Australia
[3.] Ian Holmes Imaging Center, Bio21 Molecular Science and Biotechnology Institute, University of Melbourne, Melbourne, VIC, Australia
[4.] National Center for Electron Microscopy, Molecular Foundry, Lawrence Berkeley National Laboratory, Berkeley, CA, USA
[5.] Department of Materials Science and Engineering, University of California, Berkeley, CA, USA
* Corresponding author: Emmanuel.Terzoudis-Lumsden1@monash.edu

Fast-readout pixelated detectors record diffraction patterns at each probe position in a two-dimensional (2D), atomic-resolution raster-scan across a sample (Fig. 1.a). This 4D scanning transmission electron microscopy (4D-STEM) records tremendous amounts of scattering data [1]. For qualitative and quantitative analysis, phase contrast methods such as ptychography [2] and differential phase contrast (DPC) [3] have been widely adopted. These methods often assume the phase object approximation, restricting their application to very thin or weakly scattering samples. However, recent works have shown ways to tackle thicker samples – multislice ptychography [4], 3D DPC [5], and scattering matrix (S-matrix) inversion [6]. We focus here on the S-matrix, an operator describing the elastic scattering within a sample acting on the entrance-surface wavefunction to give the exit-surface wavefield [7].

It was recently shown that, having determined the S-matrix, 3D structural information about the sample can be elucidated via through-focal parallax reconstruction [8]. In this presentation, we explore the depth resolution of this technique, including the impact of sample thickness (and resultant added multiple scattering) and convergence angle on the ideal depth resolution, and the further limitations due to shot noise arising from the operative dose level.

A mathematical equivalence between the parallax reconstruction and an imaging geometry reminiscent of scanning confocal electron microscopy (SCEM) [9], but with a hypothetical phase-sensitive detector ("phase-SCEM", Fig. 1.b), facilitates exploration of the parameter space absent factors such as shot noise and phase reconstruction artefacts. Figures 1.c-h show phase-SCEM simulations for both a lateral and defocus scan across an isolated Bi atom (c,d), and with a Bi substitutional dopant embedded in an Si [001] crystal of varying thickness (e-h). The top and bottom rows assume probe-forming semi-angles of 20 and 30 mrad respectively, and the improved depth resolution arising from the latter is evident.

Experimental realisation through 4D-STEM, S-matrix inversion and parallax reconstruction will be further impacted by measurement noise and the reliability of the phase retrieval used. Simulated results assuming a dose of 100 C/cm^2 (6.25x10^4 e$^-$/Å^2) in a 4D-STEM dataset at a single defocus and an otherwise identical sample geometry to Figs. 1g,h are shown in Figs. 1i,j. Perturbations resulting from the noise are observed, but the reconstructions and idealised data visually agree well, and have similar phase ranges. Subtraction between the doped and undoped columns (shown as defocus line scans in Figs. 1k,l) reveals the profiles for all cases are generally in good qualitative agreement: the depth resolution achievable is not appreciably changed by the dynamical scattering in the crystal or the noise [10].

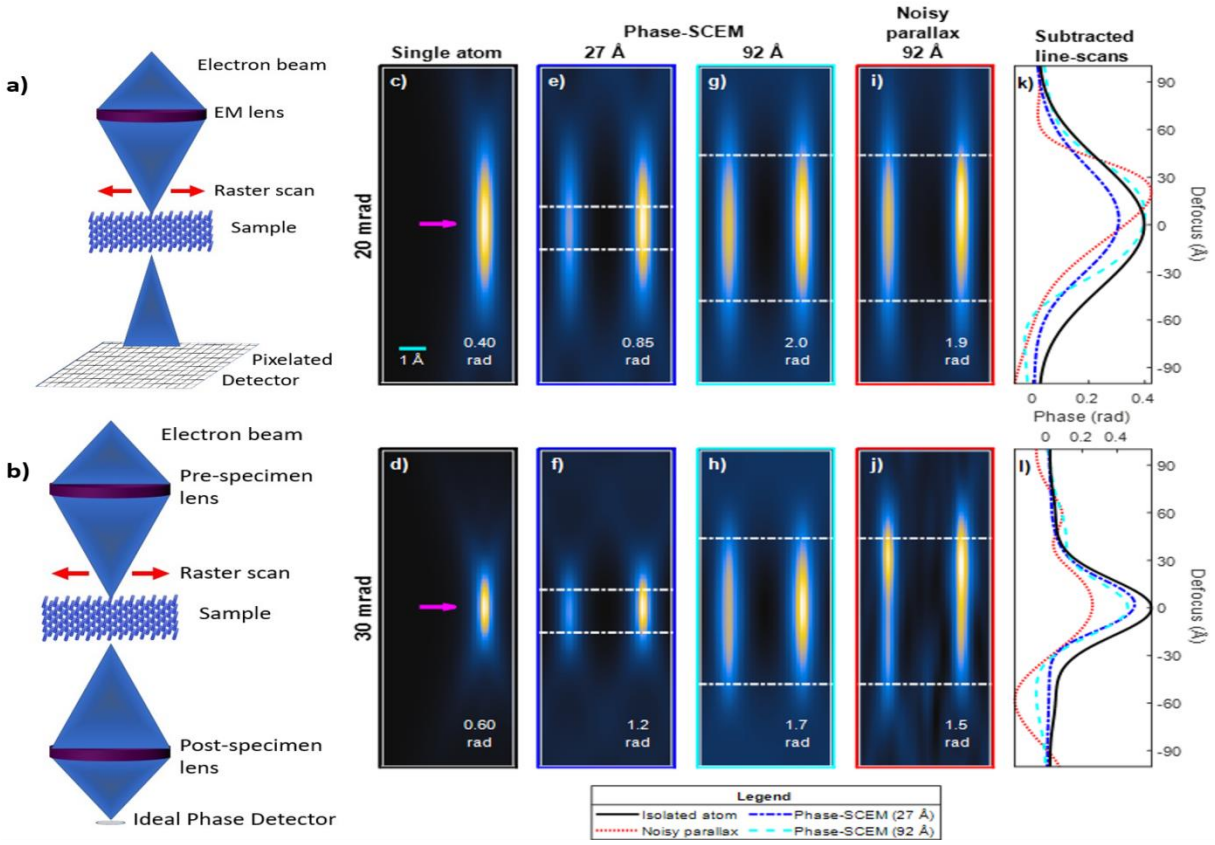

Figure 1. a,b) STEM and SCEM schematics respectively. c,d) Through-focal phase-SCEM calculations for an isolated Bi atom. e-h) As per c,d, but with a Bi dopant substituted in the centre of the right-hand Si column, and an un-doped Si column on the left. i,j) Parallax reconstructions from S-matrix determination from simulated noisy 4D data. In c-j, the magenta arrow indicates the Bi atom depth, the dotted white lines mark the crystal surfaces, and the inset numbers denote the phase range of each image. k,l) Defocus line scan differences through the centre of the doped and undoped columns in c-j.

References:

[1] C. Ophus, Microsc. Microanal. **25** (2019), p. 563
[2] J. Rodenburg and A. Maiden in "Springer Handbook of Microscopy", Eds. P.W. Hawkes and J.C.H. Spence, (Springer, Cham) p. 819
[3] K. Müller, et al., Nat. Commun. **5** (2014), p. 1
[4] A. Maiden, M. Humphrey and J. Rodenburg, J. Opt. Soc. Am. A **29** (2012), p. 1606
[5] E.G. Bosch and I. Lazić, Ultramicroscopy **207** (2019), p. 112831
[6] H.G. Brown, et al., Phys. Rev. Lett. **121** (2018), p. 266102
[7] L. Sturkey, Proc. Phys. Soc. **80** (1962), p. 321
[8] C. Ophus, et al., Microsc. Microanal. **25**(S2) (2019), p. 10-11
[9] P.D. Nellist et. al., Microsc. Microanal. **14** (2008), p. 82
[10] This research was supported under the Australian Research Council's Discovery Projects funding scheme (Project FT190100619). E.W.C.T-L acknowledges support through an Australian Government Research Training Program Scholarship.

https://doi.org/10.1017/S1431927622002331 Published online by Cambridge University Press